Activation of ultrasound enhanced persulfate oxidation by biogenic nanosilvers for degradation of 4-nitroaniline

Mohammad Malakootian[a,b], Mohammad Ahmadian[c,d,*], Mehrdad Khatami[c]

[a]*Environmental Health Engineering Research Center, Kerman University of Medical Sciences, Kerman, Iran, email: m.malakootian@yahoo.com*
[b]*Department of Environmental Health, School of Public Health, Kerman University of Medical Sciences, Kerman, Iran*
[c]*NanoBioElectrochemistry Research Center, Bam University of Medical Sciences, Bam, Iran, Tel./Fax: +98 34 44219415;*
emails: moh.ahmadian@yahoo.com (M. Ahmadian); mehrdad7khatami@gmail.com (M. Khatami)
[d]*Department of Environmental Health, School of Public Health, Bam University of Medical Sciences, Bam, Iran*

ABSTRACT

Aromatic amines such as 4-nitroaniline (4-NA) are commonly released into the environment by wastewaters containing azo colors. In the present study, silver nanoparticles were synthesized using the extract of Damask rose. Then, its physicochemical properties were determined. The effects of parameters such as pH, contact time, persulfate (PS) concentration, and nanosilver (NS) concentration on 4-NA removal were studied by a cylindrical reactor placed in ultrasound (US) device. The results showed that the efficiency of 4-NA removal by the US/PS/NS process increased with increasing the dose of NS and PS, as well as the contact time. pH had no significant effect on the removal efficiency even though in acidic pHs the removal efficiency was 5% higher. Also, over time, the pH of the reactor decreased due to the reactions occurring; this caused the same efficiency at different pHs. In the US/PS/NS process, increasing the initial 4-NA concentration also reduced the efficiency slightly. Under the optimal conditions, including pH = 5, contact time = 90 min, US power = 60 W, NS concentration = 300 mg/L, and PS concentration = 1.68 mM, the US/PS/NS process could reduce 4-NA up to 93%.

Keywords: Ultrasonic irradiation; Persulfate; AOPs; 4-nitroaniline; Silver nanoparticles

1. Introduction

The nitroanilines are aromatic amines that are usually produced during anaerobic processes in sewages containing azo colors. 4-nitroaniline (4-NA) is a type of nitroanilines, which is highly toxic and has harmful effects on the environment and living organisms. This pollutant is classified as primary pollutants by the United States Environmental Protection Agency (USEPA) [1,2]. This compound, which is a synthetic precursor for several drugs, paints, and pesticides, is very toxic and can enter various organs of the human body. It has been observed in various animal studies that this compound is teratogenic and highly toxic for reproduction. It mainly settles in soil and water sources and its

clean-up from environments contaminated is very difficult [3–5]. Several methods such as physical, chemical and biological processes have recently been used to treat 4-NA from aqueous solutions [6,7]. However, most commonly used chemical and physical methods for removing 4-NA are costly and environmentally unfriendly, as they usually cannot remove the adequate amount of the pollutants and destroy it. In some cases, the physical absorption process leads to the production of other pollutants in the environment and, in fact, causes the transmission of pollutants from one phase to another [8–12]. Conventional and advanced biological methods have many problems for the treatment of this pollutant due to the high toxicity and antimicrobial properties of 4-NA; moreover, 4-NA is a chemical stable compound which

* Corresponding author.

cannot be biodegraded [13–16]. Therefore, it is very difficult to clean the wastewater polluted by 4-NA. Advanced oxidation processes (AOPs) have been investigated in recent years by many researchers for the destruction and degradation of hazardous wastes [17,18]. Generally, AOPs are new methods that are based on the production of hydroxyl radical (OH•). The persulfate (PS) anion is the most powerful oxidant that today is considered by researchers as an AOP. The standard redox potential of sulfate radical is between 2.5–3.1 V, which is higher than that of OH• radicals (1.9–2.7 V). One of the characteristics of this material is high radical production stability, low cost, high solubility, ease of displacement due to its solid form, and non-selective oxidation [18,19]. According to studies on PSs, it is investigated that the degradation rate and activity of PS are low at room temperature. In various studies, the effect of different factors on increasing the reaction rate of PS has been investigated, which include the use of ultraviolet light, intermediate metals, nanoparticles, etc. [20–23]. The use of ultrasonic waves is one of the advanced oxidation methods applied to decompose and degrade pollutants. When water is subjected to ultrasonic waves with different frequencies, it causes cavitation phenomena. Due to this phenomenon, the formation, growth, and collapse of tiny bubbles occur in the water. When the bubbles collapse, local pressure and temperature can increase significantly, leading to the production of free radicals. The oxidizing species in the ultrasonic process include $O_2^{•-}$, •OH and •H [19,24,25]. The ultrasonic waves combined with PS can accelerate the production of sulfate radicals and increase the process efficiency in removing pollutants (Eq. (1)). Also, the use of heat, H_2O_2, microwave waves and nanoparticles increase the production of sulfuric radicals which increase the process of removing pollutants (Eqs. (1)–(5)) [19,26–29].

$$S_2O_8^{2-} \xrightarrow{US} 2SO_4^{-•} \tag{1}$$

$$S_2O_8^{2-} + 2H_2O \xrightarrow{OH} 3SO_4^{2-} + SO_4^{-•} + O_2^{-•} + 4H^+ \tag{2}$$

$$S_2O_8^{2-} \xrightarrow{heat} 2SO_4^{-•} \tag{3}$$

$$S_2O_8^{2-} \xrightarrow{hv} 2SO_4^{-•} \tag{4}$$

$$S_2O_8^{2-} + Me^{n+} \rightarrow SO_4^{-•} + Me^{(n+1)} + SO_4^{2-} \tag{5}$$
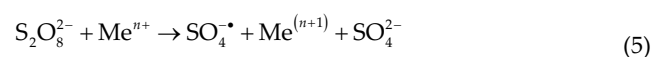
Nanoparticles have been used as a very suitable and powerful new catalyst for the complete degradation of undesirable pollutants in the liquid and gaseous phase in combination with other processes [30]. There are different chemicals and physical methods for the synthesis of the nanoparticles [31,32]. High cost and need to use chemical materials are two major disadvantages of chemical methods [33,34]. Therefore, the purpose of the present research was to synthesize bio-based silver nanoparticles using Damask rose extract, which is cost-effective in terms of energy and cost, and is less costly than the chemical method and does not require organic solvents for synthesis [35]. They are also much more stable than chemical nanoparticles [36,37].

For this purpose, the biological synthesis of silver nanoparticles using Damask rose extract was investigated as a biological resource with abundant access in Kerman Province, Iran. Then, ultrasonic waves were combined with PSs activated with the biosynthetic nanoparticles to increase the efficiency of 4-NA removal.

2. Materials and methods

2.1. Materials and reagents

Chemicals including methanol, sodium persulfate, silver nitrate, hydrochloric acid, sodium hydroxide, 4-NA, and deionized water used in this study were purchased from Merck (Germany). All chemicals and solutions were of analytical grade. The instruments included the Scintigraphy UV spectrophotometer manufactured by Analyticgena, Germany, February Infrared Spectroscopy, centrifuges, FTIR 27 Tensor, X-ray Spectrometry, Panalitical, X PERTPRO, Carl ZEISS, dispersion device dynamic light (Malvern Zetasizer), digital scale, pH meter, ultrasonic bath, air pump and magnetic stirrer spectrophotometer (UV/Vis).

2.2. Synthesis of biogenic nanosilver

First, a 0.1 molar stock of silver nitrate was prepared by dissolving 0.849 g of silver nitrate in 50 mL of deionized water. Throughout the test, the stoke solution was kept at 4°C and in the dark. The synthesis of the silver nanoparticles was used to produce a final concentration of 1 mM from silver nitric acid. In this way, 15 mL of the sample was added to 30 mL of deionized water (reaction mixture) and then the following formula (Eq. (6)) was calculated for the initial nitric acid stock solution required for the final concentration of 1 mM, and added to the reaction mixture. Silver nitrate was added to the control sample. The samples were stored at 28°C and kept in the dark.

$$C_1V_1 = C_2V_2 \tag{6}$$

where C_1 and C_2 are the initial (0.1 molecular stoke), and the final concentrations of silver ion in the reaction. V_1 is the required volume of the initial stock and V_2 is the final volume of the reaction mixture. In the reaction mixture with a final volume of 45.45 mL, the required volume of silver nitrate from the original stock was obtained 450 μM for the preparation of a reaction mixture with a final concentration of 1 mM.

2.3. Determination of biogenic nanosilver characterizations

The synthesized silver nanoparticles were examined using a UV visible spectrophotometer Scan Drop by Analyticgena Co., (Germany), at a wavelength of 300–800 nm at different times. The February Infrared Spectroscopy was used to determine the bioactive functional groups in the biological sample that are responsible for decreasing Ag^+ to $Ag°$. To prepare a powder sample, 10 mL of the sample was centrifuged for 10 min at 6,000 rpm, and it was dried for 48 h after discharging the supernatant at 60°C. For the analysis of the obtained powder, the FTIR 27 Tensor (manufactured

by Germany) was used. X-ray diffraction (XRD) analysis was done to check the presence of the silver crystals. To prepare a powder sample, 150 mL of the sample was centrifuged at 12,000 rpm for 10 min, and the upper solution was removed, and then the residual sediment was raised to 60 mL again using deionized water. This process was repeated 3 times and the remaining deposition was dried at 30°C for 48 h. The obtained powder was analyzed using Panalytical, X PERTPRO, manufactured in the Netherlands with the angle of 2θ in the range of 20θ–80θ and the radiation of λ = 1.5405 Å. Then, by using the XRD results, the average size of the nanoparticles was calculated by Scherer's equation (Eq. (7)).

$$D = \frac{0.94\lambda}{\beta \cos\theta} \tag{7}$$

where D is the mean size of the nanoparticles and λ is the wavelength of the X-rays. β is the maximum width and θ is the diffraction angle.

A transmitted electron imaging (TEM) was performed to measure the size, morphology, and distribution of the synthesized silver nanoparticles. To prepare the sample, 10 mL of the sample was ultrasonically aged for 5 min. Then, less than one drop was poured on carbon-treated film and dried at room temperature without any heat. Finally, it was checked with the Carl ZEISS machine from Germany. The average and distribution of the silver nanoparticle colloid synthesized in a liquid medium were studied using a light dynamic diffusion apparatus (Zetasizer Malvern).

2.4. Experimental set up for the ultrasound/PS/nanosilver process

The experimental setup used in this study has been shown in Fig. 1. The reaction chamber consisted of a 500 mL container placed inside the ultrasonic apparatus. The reactor contents were mixed in the reaction chamber. All experiments were performed at ambient temperature (25°C ± 1°C) and cooling system was used to reduce the temperature of the reaction chamber to 25°C. Ultrasound (US) wave value

in all experiments was fixed with a power of 550 W and a constant frequency of 60 Hz. The 4-NA stock solution was prepared using fresh deionized water before each run. Next, 200 mL of 4-NA solution was poured into the chamber in each flask, and PS and nanosilver (NS) with a specific concentration at the beginning of each run were added to the reaction chamber. After the time required for the reaction, 2 mL of the contents was taken from the reactor and poured through a 0.22 μ filter. Then, the residual 4-NA concentration was measured by a spectrophotometer (Shimadzu, Japan) at a wavelength of 381 nm. Finally, the removal efficiency was calculated by Eq. (8).

$$\text{4-NA removal efficiency}\left(\%\right) = \frac{A_0 - A}{A_0} \times 100\% \tag{8}$$

where A_0 = sample absorption rate before testing; A = sample absorption rate after the test.

The effective parameters in the US/PS/NS process were studied separately including pH, contact time, PS concentration, and NS concentration in the removal of 4-NA. To study the changes in the removal efficiency and determine the optimum values, pH values of 3, 5, 7, 9 and 11, and contact time 20–90 min, the PS concentrations 0.84, 1.68, 2.52, 3.36 and 4.2 mM were tested. NS was also used at concentrations of 100, 200, 300, 400 and 500 mg/L, and 4-NA with initial concentrations of 10, 20, 30 and 40 mg/L.

3. Results and discussion

3.1. Characterization of NS

A change in the color of the extract to transparent reddish-brown happened immediately after the addition of silver nitrate to the Damask rose extract and it was the first visible sign of the formation of the silver nanoparticles (Fig. 2) and the spectrophotometric absorption peak of 430 nm, indicating the synthesis of silver nanoparticles. In a study by Venkatesan et al. [38], the NS has synthesized from Rosa damascena petal extract that the color of the extract

1. Ultrasonic device
2. Reactor chamber
3. Strier device
4. Cooler system
5. Persulfate & Nanosilver
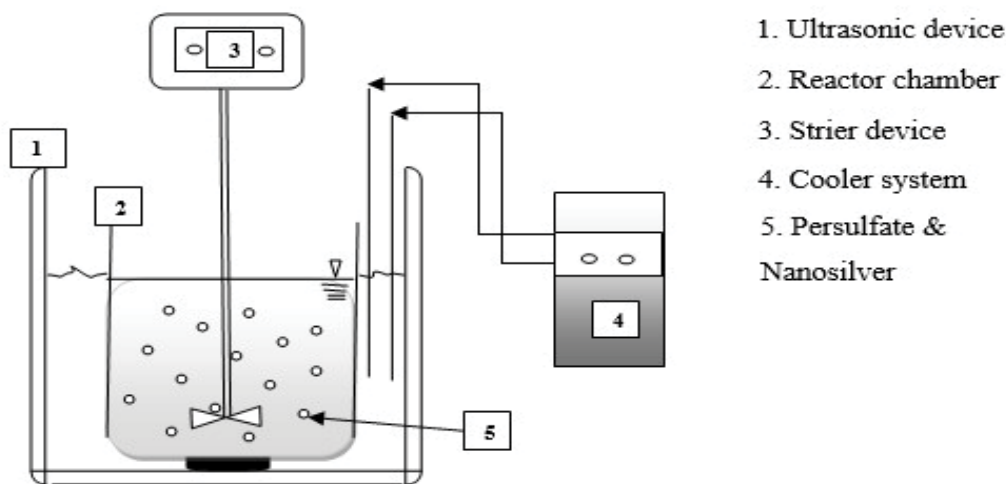
Fig. 1. Schematic of the experimental setup for the US/PS/NS process.
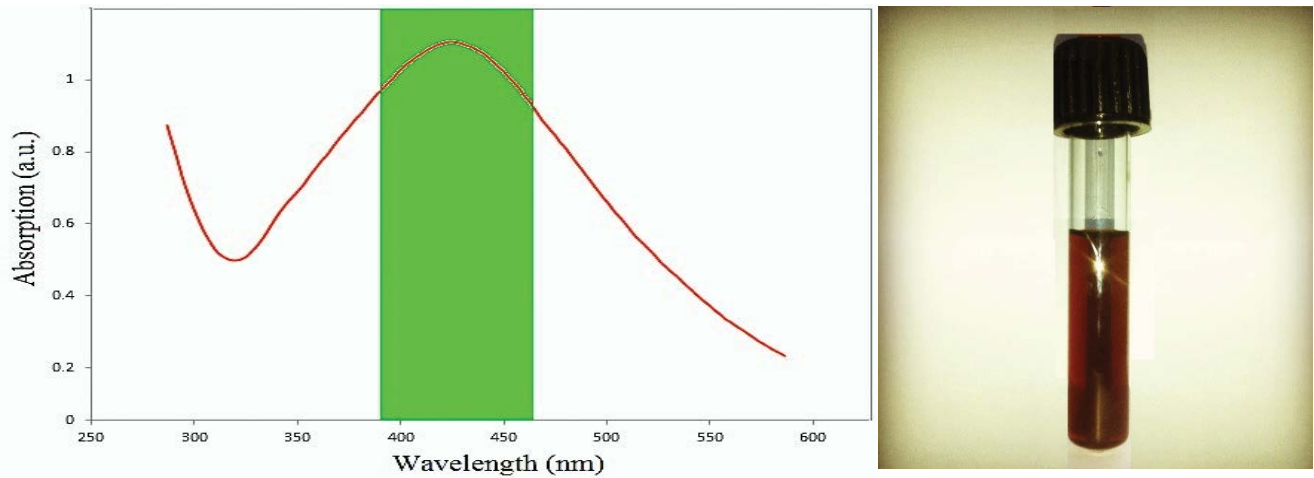
Fig. 2. Absorption spectrophotometry graph of the color change of Damask rose extract to light brown immediately after the formation of silver nanoparticles.

changed from yellow to brown and the NS absorption peak was 420 nm, which is consistent with the present study.

The XRD pattern showed four distinct peaks at angles 38.11, 44.38, 64.44 and 77.42, respectively, related to surfaces 111, 200, 220, and 311 (Fig. 3), which proves the formation of the crystalline structure of the silver nanoparticles. The results of the TEM analysis have been shown in Fig. 4. The TEM showed the shape of the spherical silver nanoparticles. The images clearly show that the diameter of nanoparticles was in the range of 5–40 nm with an average particle size of 20 nm. The results of the TEM and XRD analyses were also very similar to Venkatesan et al. [38] study.

3.2. Effect of reaction parameters on the removal of 4-NA by the US/PS/NS process

3.2.1. Effect of pH

The effect of pH on the US/PS/NS process has been shown in Fig. 5. To investigate the effect of pH on the removal of 4-NA during the US/PS/NS process, 200 mL of the 4-NA solution with an initial concentration of 30 mg/L was injected into the reactor. In the next step, the solution pH was adjusted to 3, 5, 7, 9 and 11. The concentrations used for the effective parameters in the US/PS/NS process in all steps of the experiment were determined from the same literature review and based on the values used in these papers [39–42]. In all stages of the experiment, one of the parameters was variable and other parameters were fixed.

As it is clear, the process efficiency at acidic pHs was slightly higher than alkaline pHs. Generally, the highest removal efficiency in the US/PS/NS process was obtained at pH 3 and 5; hence, pH 5 was selected as the optimal value. The efficiency of 4-NA degradation at acidic pH (3 to 5) was 94.4%, but its decomposition rate in alkaline pH declined to about 90%. Based on Eq. (9), the sulfate radicals are scavenged at high pHs by $^{\bullet}$OH (Eq. (9)).

$$SO_4^{-\bullet} + {}^{\bullet}OH \rightarrow HSO_4^- + 0.5O_2 \qquad (9)$$

Also, $SO_4^{-\bullet}$ is converted to $^{\bullet}$OH under alkaline conditions (Eq. (10)). Thus, the potential for radical hydroxyl oxidation may decrease by increasing pH [19].

$$SO_4^{-\bullet} + H_2O \rightarrow SO_4^{2-} + {}^{\bullet}OH + H^+ \qquad (10)$$

According to Eq. (10), H^+ ions are produced which can lead to the reduction of solution pH. Also, because of using the ultrasonic waves, HSO_4^- is dissociated by these waves and release the H^+ ions, which further reduce the pH of the solution (Eq. (11)).

$$HSO_4^- \rightarrow SO_4^{2-} + H^+ \qquad (11)$$

Therefore, during experiments at different pHs, the pH tends to be acidic (optimized pH), which can justify close-to-efficiency processes at all pH levels [24].

3.2.2. Effect of reaction time

The effect of contact time on the US/PS/NS process has been shown in Fig. 6. Thus, 400 mL of the 4-NA solution with an initial concentration of 30 mg/L was prepared. In the next step, all effective parameters were fixed and, every 10 min, the remaining 4-NA was measured.

As shown in Fig. 6, the process efficiency increased by increasing the contact time. The efficiency of 4-NA removal in the US/PS/NS process reached 94% for 90 min of contact time, and then the efficiency slightly increased until the contact time of 110 min was fixed. Therefore, the contact time of 90 min was considered as the optimal value. The results indicate that, over time, the percentage of removing 4-NA increased, because more $^{\bullet}$OH and $SO_4^{-\bullet}$ radicals are formed. The reason for this phenomenon is that ultrasonic waves react with molecules of water to produce more radicals. Also, the catalytic effect of NS tries to accelerate the production of these radicals. NS plays a catalytic role for the activation of PS based on Eq. (5). Silver is introduced into electron transport reactions to produce sulfate radicals based
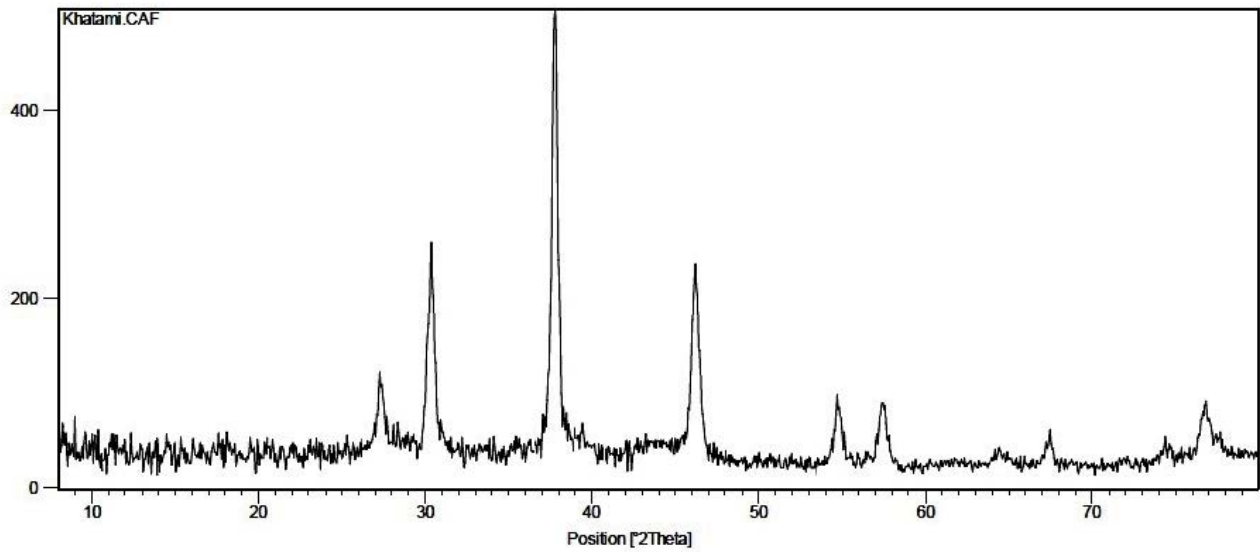
Fig. 3. X-ray diffraction pattern for NS.
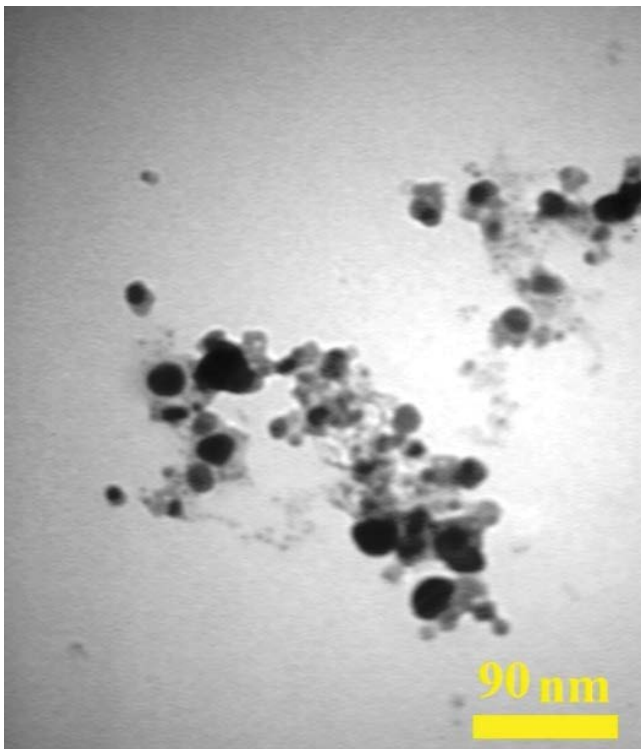
Fig. 4. Transmission electron image of the shape and formation of silver nanoparticles.

on Eq. (12) and, at higher contact times, the more number of sulfate radicals are produced [40–42].

$$S_2O_8^{2-} + Ag^+ \rightarrow Ag^{2+} + SO_4^{2-} + SO_4^{-\bullet} \tag{12}$$

On the other hand, the efficiency of the process increased after passing 80 min of contact time and eventually a steady gradient was found. The reason is the rapid decomposition of
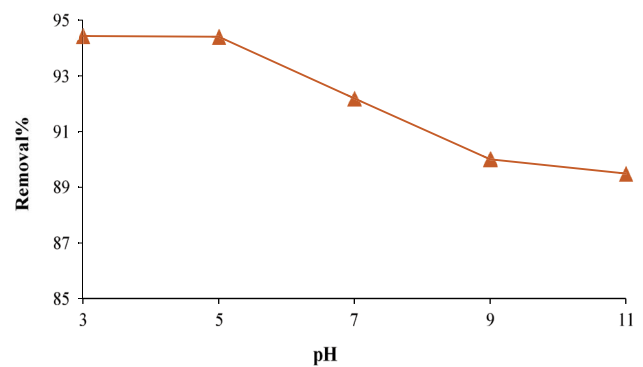
Fig. 5. Effect of pH on the removal of 4-NA by US/PS/NS process (experiment conditions: 4-NA concentration: 30 mg/L, PS concentration: 2.52 mM, NS concentration: 300 mg/L, US frequency: 60 Hz, contact time: 90 min, pH: different).
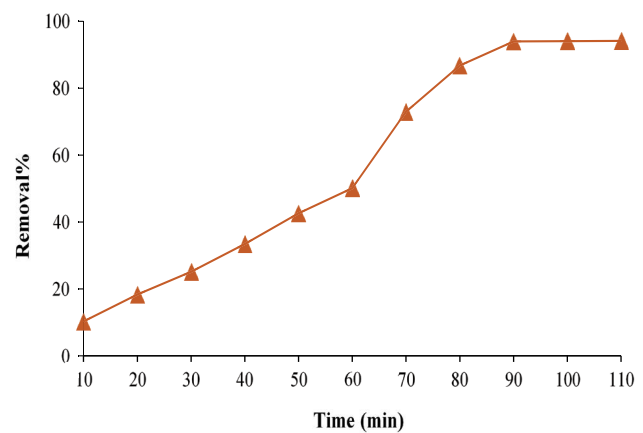
Fig. 6. Effect of contact time on the removal of 4-NA by US/PS/NS process (experiment conditions: 4-NA concentration: 30 mg/L, PS concentration: 2.52 mM, NS concentration: 300 mg/L US frequency: 60 Hz, pH: 5, contact time: different).

aniline in the early stages of the process and, over time, intermediate organic compounds are formed due to the decomposition of 4-NA. A fraction of the OH and SO$_4^{-\bullet}$ radicals will be used for the decomposition of these compounds, which will ultimately lead to a reduction in the process efficiency [19,24,25,39].

3.2.3. Effect of PS concentration

The effect of different PS concentrations on the US/PS/NS process is presented in Fig. 7. Thus, 200 mL of the 4-NA solution with an initial concentration of 30 mg/L was prepared. In the next step, the pH of the solution was adjusted to 5 and other parameters were fixed. As shown in Fig. 7, the efficiency of 4-NA removal increased rapidly with increasing the concentration of PS from 0.84 to 1.68 mM. After 90 min contact time, the 4-NA removal efficiency was about 92% when the PS concentration was 1.68 mM. However, by increasing concentrations of PS from 1.68 to 4.2 mM, the removal efficiency increased slightly. Therefore, the rates of 4-NA removal efficiency at concentrations of 2.52, 3.36 and 4.2 mM were 94%, 95.5%, and 96%, respectively. As can be seen, the efficiency of the US/PS/NS process changed slightly with increasing PS concentration and increasing the PS concentration from 1.68 to 4.2 mM, the efficiency increased only 4%. Based on whatever mentioned above, 1.68 mM PS was considered as the optimum amount for the US/PS/NS process. In fact, increasing the concentration of PS increased the number of sulfate radicals, thereby increasing the process efficiency. However, a further increase in PS to more than optimum range resulted in the production of additional radicals, which are based on Eqs. (13) and (14) could play a scavenger role in sulfate radicals.

$$SO_4^{-\bullet} + S_2O_8^{2-} \rightarrow 2SO_4^{-} + S_2O_8^{2-\bullet} \tag{13}$$

$$SO_4^{-\bullet} + SO_4^{-\bullet} \rightarrow S_2O_8^{2-} \tag{14}$$

Therefore, a rise in the amount of PS more than optimum value had a very small effect on the removal efficiency of 4-NA removal [28,38].

3.2.4. Effect of NS concentration

To investigate the effect of initial NS concentration on the 4-NA removal efficiency during the US/PS/NS process, 200 mL of 4-NA solution with an initial concentration of 30 mg/L was prepared. Then, all effective parameters were fixed and the NS concentration was variable. As shown in Fig. 8, the process efficiency increased by increasing NS concentration. With raising concentration from 100 to 200 mg/L, the removal efficiency increased slowly. At a concentration of 300 to 500 mg/L, the removal efficiency increased very faster. As can be seen in Fig. 8, the removal efficiency went up very little when the concentrations higher than 300 mg/L were tested. Therefore, 300 mg/L was selected as the optimum NS concentration. NS acts as a catalyst in the US/PS/NS process and, due to the increased number of active sites and increased free-electron production, a further increase in its concentration leads to more generation of hydroxyl
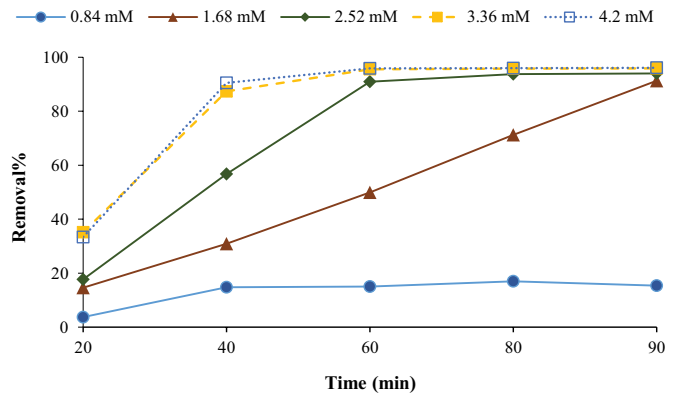
Fig. 7. Effect of PS concentration on the removal of 4-NA by US/PS/NS process (experiment conditions: 4-NA concentration: 30 mg/L, NS concentration: 300 mg/L, US frequency: 60 Hz, pH: 5, contact time: 90 min, PS concentration: different).
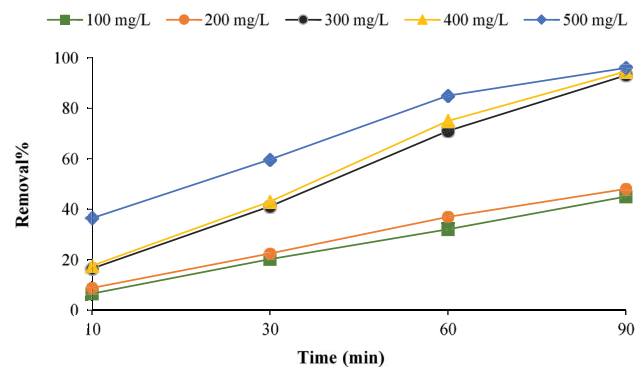
Fig. 8. Effect of NS concentration on removal of 4-NA by US/PS/NS process (experiment conditions: 4-NA concentration: 30 mg/L, PS concentration: 1.68 mM, US frequency: 60 Hz, pH: 5, contact time: 90 min, NS concentration: different).

radicals and sulfate radicals. Hydroxyl radicals and sulfate radicals produced by ultrasonic waves result in a series of chain reactions that increase the efficiency of 4-NA removal. In the study by Kamali Moghaddam et al. [43], who used the peroxydisulfate/NS process for the removal of tylosin from aqueous solitons, 400 mg/L NS was used as the optimum dosage of the catalyst under the optimum conditions. In similar studies, the removal efficiency also increased with increasing the value of the NS catalyst, which is consistent with the present study [43,44]. The stabilization of the removal efficiency of 4-NA with the further increase of the NS catalyst may also be owing to the fact that Ag$^+$ plays the role of scavenger for sulfate radicals at high concentrations [45,46].

3.2.5. Effect of initial 4-NA concentration

To study the effect of the initial concentration of 4-NA on the removal efficiency during the US/PS/NS process, 200 mL of 4-NA solution was prepared with different initial concentrations of 10, 20, 30 and 40 mg/L when other parameters were fixed. The effect of different initial 4-NA concentration on the US/PS/NS process is presented in Fig. 9. As can be seen from this figure, with increasing the initial
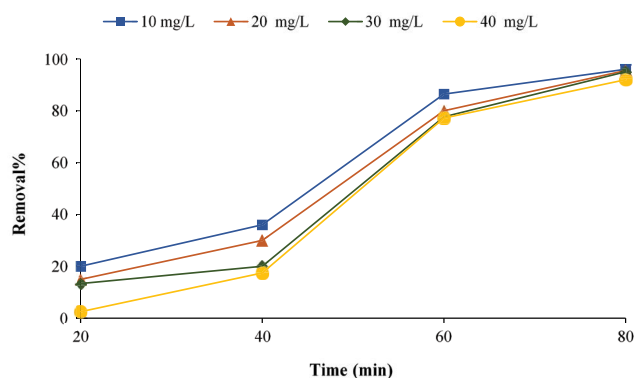
Fig. 9. Effect of initial 4-NA concentration on removal of 4-NA by US/PS/NS process (experiment conditions: PS concentration: 1.68 mM, US frequency: 60 Hz, pH: 5, contact time: 90 min, NS concentration: 300 mg/L, 4-NA concentration: different).

4-NA concentration, the removal efficiency of this process declined. But the removal efficiency decreased slightly as the concentration of 4-NA increased. The reason for this phenomenon is that the produced radicals are very strong in the US/PS/NS process. Furthermore, under the optimum conditions, this process can decompose higher concentrations of contaminants; this can be considered as an upside. A slight decrease in efficiency with increasing initial 4-NA concentration was also expected, because the number of produced active radicals, including hydroxyl radicals and sulfate radicals, improved, which is fixed by adding a certain amount of NS and PS under ultrasonic waves [19,41,42].

4. Conclusion

In the present study, NS was synthesized from Damask rose extract and combined with US processes to activate PS. It was found that the combination of NS and US waves could significantly enhance the strength of oxidation of PS and further activates more sulfate radicals. The US/PS/NS process under the optimal conditions was capable of significantly degrading 4-NA from aqueous solutions. Increasing the concentration of NS and PS to the optimal conditions increased the efficiency of 4-NA removal. The pH had no significant effect on the US/PS/NS process, but in acidic pH, the efficiency of 4-NA removal increased. Increasing the contact time also improved efficiency until it reached the optimal contact time of 90 min. Increasing the initial concentration of 4-NA also reduced efficiency. The optimum conditions of the US/PS/NS process could reduce the amount of 4-NA contamination to 93%. Since NS is synthesized from biological sources, it does not increase the number of chemicals in the environment by purified sewage and it can be regarded as an environmentally friendly catalyst.

References

[1] M. Malakootian, M.A. Gharaghani, A. Dehdarirad, M. Khatami, M. Ahmadian, M.R. Heidari, H. Mahdizadeh, ZnO nanoparticles immobilized on the surface of stones to study the removal efficiency of 4-nitroaniline by the hybrid advanced oxidation process (UV/ZnO/O$_3$), J. Mol. Struct., 1176 (2019) 766–776.

[2] A. Khalid, M. Arshad, D.E. Crowley, Biodegradation potential of pure and mixed bacterial cultures for removal of 4-nitroaniline from textile dye wastewater, Water Res., 43 (2009) 1110–1116.

[3] N. Ghaemi, S.S. Madaeni, A. Alizadeh, P. Daraei, A.A. Zinatizadeh, F. Rahimpour, Separation of nitrophenols using cellulose acetate nanofiltration membrane: influence of surfactant additives, Sep. Purif. Technol., 85 (2012) 147–156.

[4] A.G. Karunanayake, O.A. Todd, M.L. Crowley, L.B. Ricchetti, C.U. Pittman Jr., R. Anderson, T.E. Mlsna, Rapid removal of salicylic acid, 4-nitroaniline, benzoic acid and phthalic acid from wastewater using magnetized fast pyrolysis biochar from waste Douglas fir, Chem. Eng. J., 319 (2017) 75–88.

[5] F. Laghrib, W. Boumya, S. Lahrich, A. Farahi, A. El Haimouti, M.A. El Mhammedi, Electrochemical evaluation of catalytic effect of silver in reducing 4-nitroaniline: analytical application, J. Electroanal. Chem., 807 (2017) 82–87.

[6] F. Khan, J. Pandey, S. Vikram, D. Pal, S.S. Cameotra, Aerobic degradation of 4-nitroaniline (4-NA) via novel degradation intermediates by *Rhodococcus* sp. strain FK48, J. Hazard. Mater., 254 (2013) 72–78.

[7] J.-H. Sun, S.-P. Sun, M.-H. Fan, H.-Q. Guo, Y.-F. Lee, R.-X. Sun, Oxidative decomposition of *p*-nitroaniline in water by solar photo-Fenton advanced oxidation process, J. Hazard. Mater., 153 (2008) 187–193.

[8] M. Ahmadian, N. Yosefi, A. Toolabi, N. Khanjani, S. Rahimi-Keshari, A. Fatehizadeh, Adsorption of Direct Yellow 9 and Acid Orange 7 from aqueous solutions by modified pumice, Asian J. Chem., 24 (2012) 3094–3098.

[9] G. Asgari, A. Seid Mohammadi, A. Poormohammadi, M. Ahmadian, Removal of cyanide from aqueous solution by adsorption onto bone charcoal, Fresenius Environ. Bull., 23 (2014) 720–727.

[10] S.P. Moussavi, M.H. Ehrampoush, A.H. Mahvi, M. Ahmadian, S. Rahimi, Adsorption of humic acid from aqueous solution on single-walled carbon nanotubes, Asian J. Chem., 25 (2013) 5319–5324.

[11] S.P. Moussavi, M.H. Ehrampoush, A.H. Mahvi, S. Rahimi, M. Ahmadian, Efficiency of multi-walled carbon nanotubes in adsorbing humic acid from aqueous solutions, Asian J. Chem., 26 (2014) 821–826.

[12] M.T. Samadi, H. Zolghadrnasab, K. Godini, A. Poormohammadi, M. Ahmadian, S. Shanesaz, Kinetic and adsorption studies of reactive black 5 removal using multi-walled carbon nanotubes from aqueous solution, Der Pharma Chemica, 7 (2015) 267–274.

[13] K.Q. Li, Z. Zheng, X.F. Huang, G.H. Zhao, J.W. Feng, J.B. Zhang, Equilibrium, kinetic and thermodynamic studies on the adsorption of 2-nitroaniline onto activated carbon prepared from cotton stalk fibre, J. Hazard. Mater., 166 (2009) 213–220.

[14] S. Silambarasan, A.S. Vangnai, Biodegradation of 4-nitroaniline by plant-growth promoting *Acinetobacter* sp. AVLB2 and toxicological analysis of its biodegradation metabolites, J. Hazard. Mater., 302 (2016) 426–436.

[15] Y.B. Wang, Y.-n. Zhang, G.H. Zhao, M.F. Wu, M.F. Li, D.M. Li, Y.G. Zhang, Y. Zhang, Electrosorptive photocatalytic degradation of highly concentrated p-nitroaniline with TiO$_2$ nanorod-clusters/carbon aerogel electrode under visible light, Sep. Purif. Technol., 104 (2013) 229–237.

[16] W.M. Wu, R. Lin, L.J. Shen, R.W. Liang, R.S. Yuan, L. Wu, Visible-light-induced photocatalytic hydrogenation of 4-nitroaniline over In$_2$S$_3$ photocatalyst in water, Catal. Commun., 40 (2013) 1–4.

[17] M.R. Heidari, M. Malakootian, Removal of cyanide from synthetic wastewater by combined coagulation and advanced oxidation process, Desal. Wat. Treat., 133 (2018) 204–211.

[18] M. Ahmadian, M. Pirsahe, H. Janjani, H. Hossaini, Ultraviolet activated persulfate based AOP for MTBE decomposition in aqueous solution, Desal. Wat. Treat., 161 (2019) 269–274.

[19] L. Hou, H. Zhang, X. Xue, Ultrasound enhanced heterogeneous activation of peroxydisulfate by magnetite catalyst for the degradation of tetracycline in water, Sep. Purif. Technol., 84 (2012) 147–152.

[20] Y.G. Adewuyi, N.Y. Sakyi, Removal of nitric oxide by aqueous sodium persulfate simultaneously activated by temperature

and Fe²⁺ in a lab-scale bubble reactor, Ind. Eng. Chem. Res., 52 (2013) 14687–14697.

[21] Z. Frontistis, E.M. Mestres, I. Konstantinou, D. Mantzavinos, Removal of cibacron black commercial dye with heat- or iron-activated persulfate: statistical evaluation of key operating parameters on decolorization and degradation by-products, Desal. Wat. Treat., 57 (2016) 2616–2625.

[22] M. Kamagate, A. Amin Assadi, T. Kone, L. Coulibaly, K. Hanna, Activation of persulfate by irradiated laterite for removal of fluoroquinolones in multi-component systems, J. Hazard. Mater., 346 (2018) 159–166.

[23] H. Lee, H.-i. Kim, S. Weon, W. Choi, Y.S. Hwang, J. Seo, C. Lee, J.-H. Kim, Activation of persulfates by graphitized nanodiamonds for removal of organic compounds, Environ. Sci. Technol., 50 (2016) 10134–10142.

[24] C. Cai, L. Wang, H. Gao, L. Hou, H. Zhang, Ultrasound enhanced heterogeneous activation of peroxydisulfate by bimetallic Fe-Co/GAC catalyst for the degradation of Acid Orange 7 in water, J. Environ. Sci., 26 (2014) 1267–1273.

[25] C. Cai, H. Zhang, X. Zhong, L. Hou, Ultrasound enhanced heterogeneous activation of peroxymonosulfate by a bimetallic Fe–Co/SBA-15 catalyst for the degradation of Orange II in water, J. Hazard. Mater., 283 (2015) 70–79.

[26] F. Liu, P. Yi, X. Wang, H. Gao, H. Zhang, Degradation of Acid Orange 7 by an ultrasound/ZnO-GAC/persulfate process, Sep. Purif. Technol., 194 (2018) 181–187.

[27] R. Molina, F. Martínez, J.A. Melero, D.H. Bremner, A.G. Chakinala, Mineralization of phenol by a heterogeneous ultrasound/Fe-SBA-15/H₂O₂ process: multivariate study by factorial design of experiments, Appl. Catal., B, 66 (2006) 198–207.

[28] C.-H. Weng, K.-L. Tsai, Ultrasound and heat enhanced persulfate oxidation activated with Fe⁰ aggregate for the decolorization of C.I. Direct Red 23, Ultrason. Sonochem., 29 (2016) 11–18.

[29] H. Zhang, L. Duan, Y. Zhang, F. Wu, The use of ultrasound to enhance the decolorization of the C.I. Acid Orange 7 by zero-valent iron, Dyes Pigm., 65 (2005) 39–43.

[30] M. Khatami, H. Alijani, M. Nejad, R. Varma, Core@shell nanoparticles: greener synthesis using natural plant products, Appl. Sci., 8 (2018) 411.

[31] K. Karthik, S. Dhanuskodi, C. Gobinath, S. Prabukumar, S. Sivaramakrishnan, Multifunctional properties of CdO nanostructures synthesised through microwave assisted hydrothermal method, Mater. Res. Innovations, 23 (2018) 1–9.

[32] P. Singh, Y.-J. Kim, D. Zhang, D.-C. Yang, Biological synthesis of nanoparticles from plants and microorganisms, Trends Biotechnol., 34 (2016) 588–599.

[33] M.R. Heidari, R.S. Varma, M. Ahmadian, M. Pourkhosravani, S.N. Asadzadeh, P. Karimi, M. Khatami, Photo-Fenton like catalyst system: activated carbon/CoFe₂O₄ nanocomposite for reactive dye removal from textile wastewater, Appl. Sci., 9 (2019) 963.

[34] S.S.R. Gupta, M.L. Kantam, B.M. Bhanage, Shape-selective synthesis of gold nanoparticles and their catalytic activity towards reduction of *p*-nitroaniline, Nano-Struct. Nano-Objects, 14 (2018) 125–130.

[35] Z.U.H. Khan, A. Khan, Y. Chen, N.S. Shah, N. Muhammad, A.U. Khan, K. Tahir, F.U. Khan, B. Murtaza, S.U. Hassan, S.A. Qaisrani, P. Wan, Biomedical applications of green synthesized noble metal nanoparticles, J. Photochem. Photobiol., B, 173 (2017) 150–164.

[36] A. Miri, M. Darroudi, R. Entezari, M. Sarani, Biosynthesis of gold nanoparticles using *Prosopis farcta* extract and its in vitro toxicity on colon cancer cells, Res. Chem. Intermed., 44 (2018) 3169–3177.

[37] A. Miri, M. Sarani, Biosynthesis, characterization and cytotoxic activity of CeO₂ nanoparticles, Ceram. Int., 44 (2018) 12642–12647.

[38] B. Venkatesan, V. Subramanian, A. Tumala, E. Vellaichamy, Rapid synthesis of biocompatible silver nanoparticles using aqueous extract of *Rosa damascena* petals and evaluation of their anticancer activity, Asian Pac. J. Trop. Med., 7S1 (2014) 294–300.

[39] P. Gayathri, R. Praveena Juliya Dorathi, K. Palanivelu, Sonochemical degradation of textile dyes in aqueous solution using sulphate radicals activated by immobilized cobalt ions, Ultrason. Sonochem., 17 (2010) 566–571.

[40] B. Lai, Z. Chen, Y. Zhou, P. Yang, J. Wang, Z. Chen, Removal of high concentration *p*-nitrophenol in aqueous solution by zero valent iron with ultrasonic irradiation (US–ZVI), J. Hazard. Mater., 250–251 (2013) 220–228.

[41] D. Ouyang, J. Yan, L. Qian, Y. Chen, L. Han, A. Su, W. Zhang, H. Ni, M. Chen, Degradation of 1,4-dioxane by biochar supported nano magnetite particles activating persulfate, Chemosphere. 184 (2017) 609–617.

[42] Y.S. Zhao, C. Sun, J.Q. Sun, R. Zhou, Kinetic modeling and efficiency of sulfate radical-based oxidation to remove *p*-nitroaniline from wastewater by persulfate/Fe₃O₄ nanoparticles process, Sep. Purif. Technol., 142 (2015) 182–188.

[43] S. Kamali Moghaddam, M.H. Rasoulifard, M. Vahedpour, M.R. Eskandarian, Kinetic study on degradation of tylosin in aqueous media using potassium peroxydisulfate in the presence of immobilized nanosilver, Desal. Wat. Treat., 57 (2016) 3552–3558.

[44] M. Malakotian, S.N. Asadzadeh, M. Khatami, M. Ahmadian, M.R. Heidari, P. Karimi, N. Firouzeh, R.S. Varma, Protocol encompassing ultrasound/Fe₃O₄ nanoparticles/persulfate for the removal of tetracycline antibiotics from aqueous environments, Clean Technol. Environ. Policy, 21 (2019) 1665–1674.

[45] V. Shashikala, V. Siva Kumar, A.H. Padmasri, B. David Raju, S. Venkata Mohan, P. Nageswara Sarma, K.S. Rama Rao, Advantages of nano-silver-carbon covered alumina catalyst prepared by electro-chemical method for drinking water purification, J. Mol. Catal. A: Chem., 268 (2007) 95–100.

[46] N. Wang, F. Xiao, J. Zhang, H. Zhou, Y. Qin, D. Pan, Spherical montmorillonite-supported nano-silver as a self-sedimentary catalyst for methylene blue removal, Appl. Clay Sci., 174 (2019) 146–151.